Permian strontium isotope stratigraphy

CHRISTOPH KORTE[1*] & CLEMENS V. ULLMANN[2]

[1]*Department of Geosciences and Natural Resource Management, University of Copenhagen, Øster Voldgade 10, 1350 Copenhagen-K, Denmark*
[2]*Camborne School of Mines and Environment and Sustainability Institute, University of Exeter, Penryn Campus, Treliever Road, Penryn, Cornwall TR10 9FE, UK*
[*]*Correspondence:* korte@ign.ku.dk

Abstract: The secular evolution of the Permian seawater $^{87}Sr/^{86}Sr$ ratios carries information about global tectonic processes, palaeoclimate and palaeoenvironments, such as occurred during the Early Permian deglaciation, the formation of Pangaea and the Permian–Triassic (P–Tr) mass extinction. Besides this application for discovering geological aspects of Earth history, the marine 87Sr/86Sr curve can also be used for robust correlations when other bio-, litho- and/or chemostratigraphic markers are inadequate. The accuracy of marine $^{87}Sr/^{86}Sr$ reconstructions, however, depends on high-quality age control of the reference data, and on sample preservation, both of which generally deteriorate with the age of the studied interval. The first-order Permian seawater $^{87}Sr/^{86}Sr$ trend shows a monotonous decline from approximately 0.7080 in the earliest Permian (Asselian) to approximately 0.7069 in the latest Guadalupian (Capitanian), followed by a steepening increase from the latest Guadalupian towards the P–Tr boundary (c. 0.7071–0.7072) and into the Early Triassic. Various higher-order changes in slope of the Permian $^{87}Sr/^{86}Sr$ curve are indicated, but cannot currently be verified owing to a lack of sample coverage and significant disagreement of published $^{87}Sr/^{86}Sr$ records.

Seawater $^{87}Sr/^{86}Sr$ ratios have varied throughout Earth's history (Peterman et al. 1970; Veizer & Compston 1974), and are mostly defined by the relative influence of unradiogenic Sr derived from Earth's mantle (mantle sources) and radiogenic Sr of the continental crust (riverine input) (Palmer & Edmond 1989; Taylor & Lasaga 1999). Owing to radioactive decay of ^{87}Rb to ^{87}Sr, both have increased from an initial ratio of 0.69897 ± 0.00003 at Earth's accretion (Hans et al. 2013) to current approximate values of 0.704 and 0.713 (Pearce et al. 2015), respectively (Fig. 1d). Secular fluctuations of the marine $^{87}Sr/^{86}Sr$ ratio, incorporated into authigenic marine sediments and hard parts of fossils, can be used as chemostratigraphic markers for global correlations (e.g. Steuber 2001, 2003; Denison et al. 2003; Burla et al. 2009; Ehrenberg et al. 2010; see also McArthur et al. 2012). This application makes use of the observations that seawater has a globally uniform $^{87}Sr/^{86}Sr$ ratio, and shows secular drifts of measureable magnitude. Globally uniform $^{87}Sr/^{86}Sr$ ratios in biominerals of marine origin (e.g. Brand et al. 2003) are observed in most fully marine settings due to mixing and the long residence time of Sr in the oceans of > 1000 kyr (e.g. Li 1982; Elderfield 1986; Veizer 1989; McArthur 1994; Pearce et al. 2015). Deviations from the marine ratios in marginal and estuarine settings can occur, however, where salinities are significantly reduced (Fig. 1c, Bryant et al. 1995;

Sharma et al. 2007), and such deviations have been inferred, for example, for the Middle Jurassic of Poland (Wierzbowski et al. 2012).

The first detailed Phanerozoic strontium isotope curve, revealing distinct fluctuations, was generated by Burke et al. (1982) using mostly whole-rock carbonate as an $^{87}Sr/^{86}Sr$ archive. This record was later successively refined for specific time intervals (e.g. DePaolo & Ingram 1985; Palmer & Elderfield 1985; Hodell et al. 1989, 1991). For the Carboniferous and Permian, additional work on the marine $^{87}Sr/^{86}Sr$ trends was carried out by Popp et al. (1986), Brookins (1988), Kramm & Wedepohl (1991) and Nishioka et al. (1991), and later reevaluated by Denison et al. (1994) and Denison & Koepnick (1995). McArthur (1994) emphasized that excellent sample preservation is crucial for high-resolution Sr isotope stratigraphy. Subsequent work on various intervals of the Phanerozoic has consequently increasingly used hard parts of organisms precipitating low-Mg calcite (LMC) (e.g. brachiopods, belemnites, oysters) or bioapatite (e.g. conodonts) that were checked for sample preservation (e.g. Jurassic: Jones et al. 1994; Triassic: Martin & Macdougall 1995; Korte et al. 2003, 2004; Permian: Martin & Macdougall 1995; Korte et al. 2004, 2006; Carboniferous: Bruckschen et al. 1999; Devonian: Diener et al. 1996; Ebneth et al. 1997; Ordovician: Shields et al. 2003). Such macrofossil remains are thought to be comparatively resistant to diagenesis

(Veizer 1989; Blake et al. 1997; Veizer et al. 1999; Zazzo et al. 2004), representing therefore the most robust available archives for past seawater $^{87}Sr/^{86}Sr$ (e.g. Veizer et al. 1997, 1999; Jenkyns et al. 2002).

Here, we review existing Permian $^{87}Sr/^{86}Sr$ data constraining the evolution of the marine $^{87}Sr/^{86}Sr$ ratio throughout this period. We discuss possible pitfalls of diagenetic alteration or local environmental influences and evaluate the data, in particular with regard to the potential stratigraphic resolution. Finally, we briefly discuss the impact of global tectonic events and environmental change on the Permian seawater $^{87}Sr/^{86}Sr$.
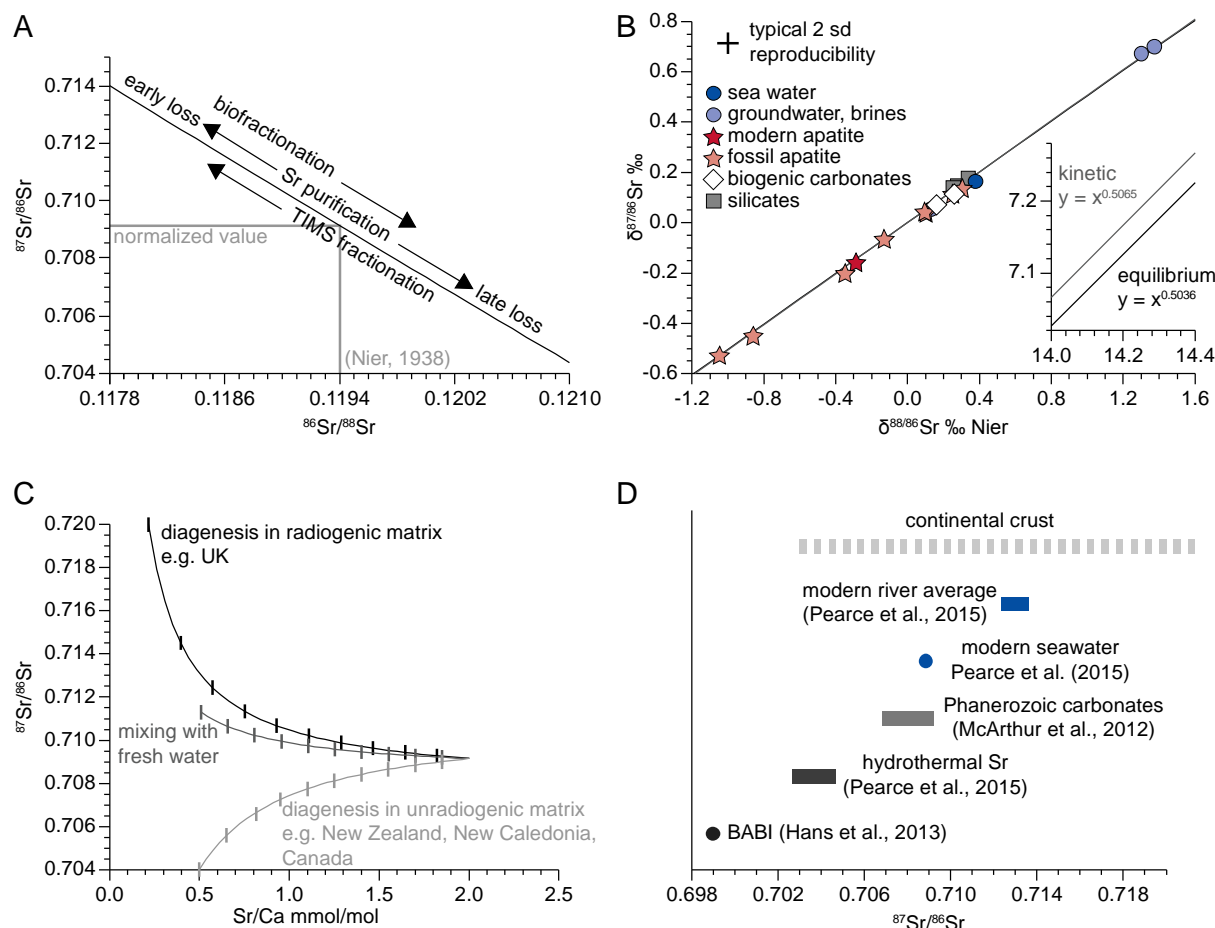

Fig. 1. Sr isotope systematics. (a) Coupled fractionation of the $^{87}Sr/^{86}Sr$ and $^{86}Sr/^{88}Sr$ ratio in various processes. Biofractionation generally enriches the biomineral in the light isotopes, leading to a lower $^{87}Sr/^{86}Sr$ but higher $^{86}Sr/^{88}Sr$ ratio. During ion-exchange chemistry in the laboratory, loss of strontium (e.g. due to too small a collection window or residual Sr on the ion-exchange resin) can lead to enrichment in the light and the heavy Sr isotopes. During thermal ionization mass spectrometry, the light Sr isotopes evaporate first from the filament and the sample successively evolves to heavier Sr isotopic composition. All of these effects can be corrected by applying a fractionation law and fixing the $^{86}Sr/^{88}Sr$ ratio of Sr at the accepted value of 0.1194 (Nier 1938). (b) $\delta^{87/86}Sr$ and $\delta^{88/86}Sr$ values of natural samples measured by Neymark et al. (2014) together with potential law equations describing equilibrium and kinetic Sr isotope fractionation computed from formulae given in Young & Galy (2004). Significant isotope fractionation is observed especially for fossil apatite and brines, but all values can be corrected using either the equilibrium or kinetic fractionation law without introduction of significant errors. Kinetic and equilibrium fractionation curves become measurably different only at large isotopic fractionation (inset). (c) Deviations from hypothetical, arbitrary marine biogenic calcite signal due to diagenesis or seawater–freshwater mixing. Depicted curves are calculated using arbitrary values of $^{87}Sr/^{86}Sr$ and Sr/Ca of end members and Sr distribution coefficients, which are partially specific to site, biomineral, calcite precipitation rate and geological interval. (d) $^{87}Sr/^{86}Sr$ ratio of selected Sr reservoirs on Earth.

Theoretical background

Physical processes during mass spectrometry, strontium loss during sample preparation in the laboratory and the biomineralization process all affect the isotopic composition of Sr (Fig. 1a). In order to correct for these fractionation effects, traditionally all measured $^{87}Sr/^{86}Sr$ ratios have been recalculated using the synchronously measured $^{86}Sr/^{88}Sr$ ratio (Fig. 1a) (Elderfield 1986). This latter ratio is assumed to be 0.1194, as measured on 99.9% pure Eimer & Amend Sr metal (Nier 1938), and later adopted and recommended for general use

by the IUGS Subcommission on Geochronology (Steiger & Jäger 1977). When this ratio is assumed to be constant, all fractionation-related deviations of $^{87}Sr/^{86}Sr$ in a sample from coeval seawater can be removed as long as the correct fractionation law is employed for calculations.

Figure 1b shows measured pairs of $\delta^{88/86}Sr$ and $\delta^{87/86}Sr$ values of natural samples (Neymark et al. 2014) analysed using a double-spike protocol so that the Nier correction for instrumental fractionation could be avoided. Also shown are fractionation curves for kinetic and equilibrium isotope fractionation of strontium calculated from equations given in Young & Galy (2004), which yield virtually the same results in the range of observed natural variations of strontium isotope ratios. It is thus evident that biological fractionation of the $^{87}Sr/^{86}Sr$ ratio can be significant (especially in apatite) but can conveniently be approximated using either a kinetic or an equilibrium fractionation law for samples with $^{87}Sr/^{86}Sr$ close to the accepted reference (NIST SRM 987, $_{87}Sr/_{86}Sr$ ¼ 0.710248: McArthur et al. 2001; see also Neymark et al. 2014). In order to generate a measurable bias through the assumption of a wrong fractionation law (at currently common levels of precision), biological fractionation effects would need to be an order of magnitude larger than those observed (see inset of Fig. 1b).

Disequilibrium effects of biomineralization that can severely complicate interpretation of other isotopic systems in biominerals (e.g. Wefer & Berger 1991 for O and C isotopes) therefore play no role in their $^{87}Sr/^{86}Sr$ ratio – an invaluable advantage.

Uncertainties in numerical age assignment and correlation

The problem of assigning precise and accurate relative and numerical ages to globally distributed samples has a direct impact on the fidelity with which the marine $^{87}Sr/^{86}Sr$ reference curve can be constrained. This problem is particularly relevant in the Permian, for which a significant lack of internal age constraint has been noted (Henderson et al. 2012). An accurate relative sample sequence can be ensured when sourcing samples from drill cores (Morante 1996), continuous successions at one locality (Sedlacek et al. 2014) or small geographical areas (Denison et al. 1994). Correlation problems of local biostratigraphic and lithostratigraphic schemes to other regions, however, are highly likely to lead to erroneous age interpretations (Denison et al. 1994; Martin & Macdougall 1995; Henderson et al. 2012). Such wrong/distorted age assignments are particularly problematic where the $^{87}Sr/^{86}Sr$ curve changes rapidly (Burke et al. 1982). Highfidelity correlation in the Permian is hampered by low faunal diversity (coarse biostratigraphic schemes) and low sea level, generating isolated basins with endemic faunas, in particular in the Late Permian (Martin & Macdougall 1995). Analysing only materials that are firmly tied by biostratigraphic schemes (e.g. conodonts: Korte et al. 2003, 2006) is currently the best way of ensuring acceptable age resolution and correlation between regions. For example, conodont biozonations of the Permian give an average age resolution of approximately 1.3 myr (Korte et al. 2006; Henderson et al. 2012). Such biozonal schemes have been integrated into a Permian Composite Standard (Henderson et al. 2012), which is an attempt at an integrated stratigraphic framework in the absence of cyclostratigraphic and high-resolution chemostratigraphic constraints. Biases of approximately 1 myr in age assignments for samples entering the Permian database are currently acceptable for most stages, because limited analytical precision of the available data and rate of change of the marine $^{87}Sr/^{86}Sr$ curve do not allow the generation of a higherresolution curve. Future research, however, should focus on improving both the fidelity of $^{87}Sr/^{86}Sr$ data and the age constraints of samples that are used for $^{87}Sr/^{86}Sr$ reference curves.

Diagenesis

Besides poor age control and contributions of nonmarine strontium to ambient water (e.g. in marginalmarine environments and estuaries), diagenetically induced alterations of the $^{87}Sr/^{86}Sr$ ratios in fossil materials constitute the largest obstacle for generating a well-defined marine $^{87}Sr/^{86}Sr$ record. Even minor alteration of LMC and bioapatite can have a significant influence on the strontium isotopes because $^{87}Sr/^{86}Sr$ ratios are measured to a great level of precision (usually ± 0.00002), while secular drifts of the marine $^{87}Sr/^{86}Sr$ curve are comparatively slow, averaging 0.000026 per myr for the last 500 myr (McArthur et al. 2012).

It is commonly considered that diagenesis leads to lower Sr concentrations in LMC (Brand & Veizer 1980) and it is often implicitly assumed that alteration leads to more radiogenic (i.e. higher $^{87}Sr/^{86}Sr$) $^{87}Sr/^{86}Sr$ ratios (e.g. Veizer & Compston 1974; Denison et al. 1994; Shields et al. 2003). While these trends usually hold, they are not universal. It has been observed that calcite cements can be rich in Sr (Ullmann et al. 2015) and that diagenesis can lead to 87Sr depletions (=lower $^{87}Sr/^{86}Sr$ ratios) in altered calcite (Fig. 1c) (Burke et al. 1982; Brand 1991; Steuber & Schlüter 2012; Ullmann et al. 2013, 2014). Two

schematic trends for diagenetic alteration of $^{87}Sr/^{86}Sr$ and Sr/Ca ratios are shown in Figure 1c together with countries in which these relative trends are observed. In order to reconstruct original seawater Sr concentrations and isotope compositions, it is necessary to take into account the specific locality and lithology patterns of diagenesis (Ullmann & Korte 2015).

Sample preservation of conodonts is assessed using the Conodont Alteration Index (CAI: Martin & Macdougall 1995; Veizer et al. 1997; Korte et al. 2003), a measure of the discoloration of conodont elements through thermal maturation of organic matter in the bioapatite (Martin & Macdougall 1995). Increases in CAI have been found to co-vary with significant changes of $^{87}Sr/_{86}Sr$ in conodonts (e.g. Veizer et al. 1997), suggesting that this alteration proxy has a good potential for excluding data of altered specimens from interpretation. Some doubts about the general suitability of conodonts for reconstructing marine $^{87}Sr/^{86}Sr$ ratios, however, have been voiced (Korte et al. 2003; McArthur et al. 2012). These doubts are fuelled by unresolvable offsets from coeval records generated on other fossil materials that might be related to early Sr exchange with the sediment matrix (Veizer et al. 1999).

Data accuracy, comparability and confidence

Strontium isotope stratigraphy relies on accurate high-precision data. Adequate sample control, laboratory processes and analytical routines are therefore of utmost importance for retrieving meaningful numerical ages from marine carbonates.

Since the 1980s, almost all laboratories use NIST SRM 987 (strontium carbonate) as the international standard for data control and to ensure interlaboratory comparability of $^{87}Sr/^{86}Sr$ data. For the purpose of comparing results from different studies, we here adjust published ratios to $^{87}Sr/^{86}Sr_{NIST\ SRM\ 987} = 0.710248$ (McArthur et al. 2001, 2012). This adjustment ensures that biases arising during the analytical process can be corrected, and data should, in theory, be accurate and comparable. It is, however, common practice to measure aliquots of pure NIST SRM 987 that have not undergone any previous laboratory processing, so that absolute values and precision of this material only relate to processes after sample dissolution and Sr purification (i.e. mass spectrometry). Contamination of samples during processing cannot be excluded when using this protocol and some of the observed disagreements between coeval $^{87}Sr/^{86}Sr$ records (see interlaboratory biases of McArthur et al. 2001, 2012) might arise from such contamination.

It is therefore encouraged to control the performance of sample processing, Sr purification and

spectrometric analysis using an additional international reference material with matrix comparable to the sample matrix (e.g. JLs-1 for carbonates: Rasmussen et al. 2016). It is further encouraged to analyse element concentrations from a split of each sample solution for preservation control (Ullmann et al. 2013, 2014; Rasmussen et al. 2016).

Permian $^{87}Sr/^{86}Sr$ trend

The published marine $^{87}Sr/^{86}Sr$ data for the Permian are plotted in Figure 2, and show a first-order long-term decreasing trend throughout the Early Permian until the late Middle Permian (Capitanian), followed by a steepening increase across the P–Tr boundary that continues throughout the Early Triassic. These overall trends have been known since the early work of, for example, Veizer & Compston (1974), Burke et al. (1982), Popp et al. (1986), Brookins (1988), Kramm & Wedepohl (1991), Nishioka et al. (1991) and Denison et al. (1994). The results of these pioneering studies were confirmed by data generated from conodonts (e.g. Martin & Macdougall 1995), and macrofossil calcite (brachiopods) screened for diagenesis and with improved biostratigraphic control (e.g. Korte et al. 2006). While the Early PermianAsselian–Sakmarian $^{87}Sr/^{86}Sr$ trend is constrained only by data from three northern hemisphere regions, the late Early (Kungurian)–Late Permian interval is covered by data from a multitude of the southern hemisphere and northern hemisphere mid- to low-palaeolatitude successions (Fig. 3).

The Asselian–Capitanian $^{87}Sr/^{86}Sr$ decrease

A decreasing $^{87}Sr/_{86}Sr$ trend that continues until the Capitanian commences in the Moscovian (Middle Pennsylvanian, c. 310 Ma: Denison et al. 1994; Bruckschen et al. 1999; McArthur et al. 2012). This trend starts from a ratio of approximately 0.7083, and reaches approximately 0.7080–0.7082 at the Carboniferous–Permian boundary (298.9 Ma) (Burke et al. 1982; Nishioka et al. 1991; Denison et al. 1994; Bruckschen et al. 1999; Korte et al. 2006; Tierney 2010). Canadian (Sverdrup Basin) and Russian (Moscow Basin) brachiopods of the Late Carboniferous (Bruckschen et al. 1999), as well as whole-rock carbonate data from the Carboniferous–Permian transition in the USA (Tierney 2010), suggest a more radiogenic value of 0.7082. Lower values of approximately 0.7080 for this boundary are supported by whole-rock carbonate data of the Akiyoshi Limestone (Nishioka et al. 1991), and well-preserved

earliest Permian brachiopods from the USA and Russia (Korte et al. 2006).

The $^{87}Sr/^{86}Sr$ decrease continues throughout the Early Permian and most of Middle Permian (Fig. 2), representing the largest sustained downwards trend of the marine $^{87}Sr/^{86}Sr$ curve in the Phanerozoic (Veizer et al. 1999; McArthur et al. 2012) and this is well documented globally (Burke et al. 1982; Nishioka et al. 1991; Denison et al. 1994; Morante 1996; Korte et al. 2006; Tierney 2010). The slope of this downwards trend is not constant through time: relatively steep intervals of the Asselian–Sakmarian and Wordian–Capitanian are separated by a more gentle decrease during the Artinskian–Roadian (Fig. 2) (Korte et al. 2006; McArthur et al. 2012). Whole-rock carbonate data from the USA

(Denison et al. 1994) even indicate a temporary increase in seawater $^{87}Sr/^{86}Sr$ in the Artinskian. The more radiogenic whole-rock data of Denison et al. (1994) may be explained by elevated Sakmarian–Roadian $^{87}Sr/^{86}Sr$ ratios of shark teeth from the USA, which have been inferred to be related to basinal restriction and a significant admixture of terrestrial radiogenic Sr (Fischer et al. 2014). Most Kungurian–Capitanian $^{87}Sr/^{86}Sr$ datasets show comparatively large data variability, but are in accord with each other regardless of the sample material analysed. Australian brachiopod data that reach extremely low values of approximately 0.7065 in the Capitanian (Morante 1996) are, however, consistently more unradiogenic than time equivalent values from elsewhere (Fig. 2).
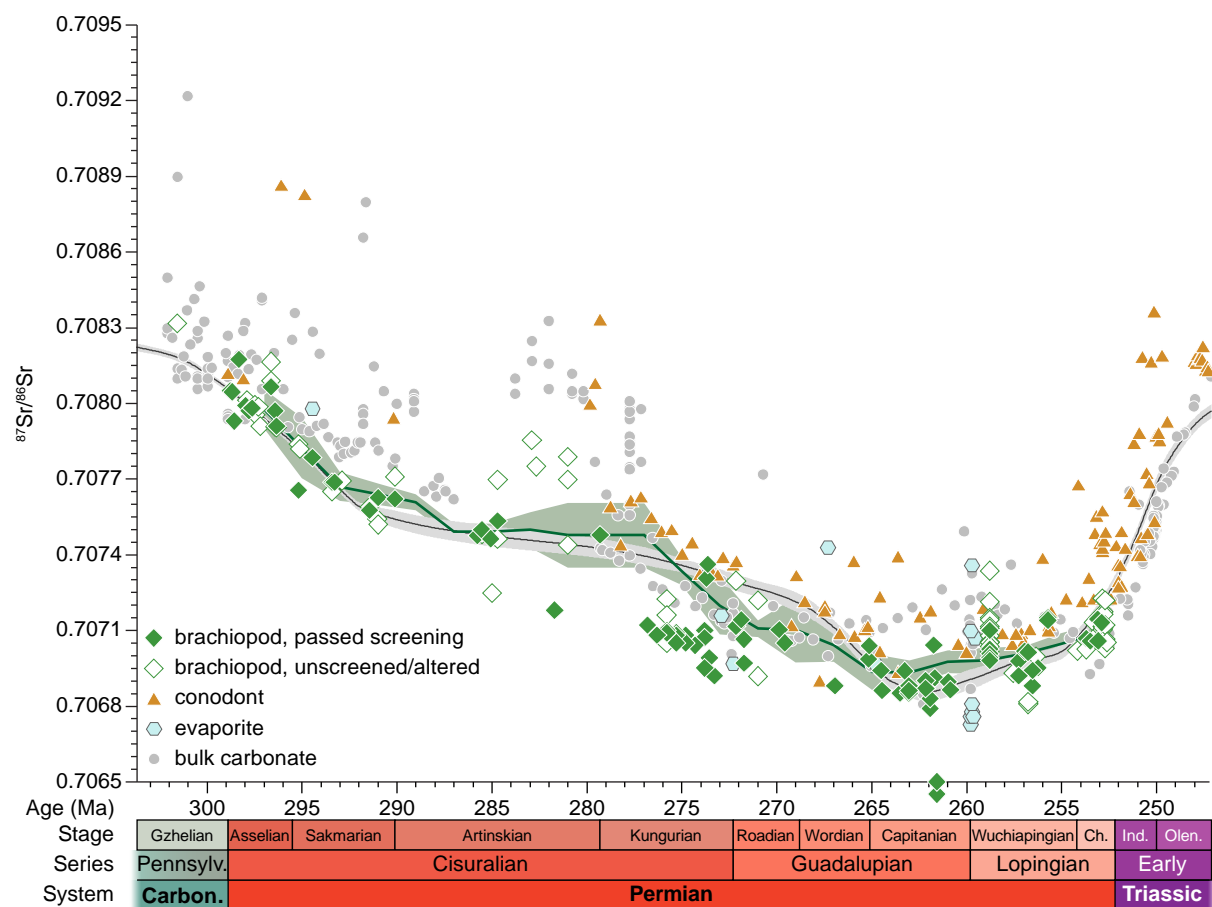

Fig. 2. Available $^{87}Sr/^{86}Sr$ data for which independent age constraints allow for robust age assignment. Grey circles, whole-rock carbonate; blue hexagons, evaporates; brown triangles, conodont elements; open diamonds, unscreened or poorly preserved brachiopods; green diamonds, brachiopod calcite that passed screening for diagenesis. Values taken from Veizer & Compston (1974), Denison et al. (1994), Martin & Macdougall (1995), Morante (1996), Korte et al. (2003, 2004, 2006), Tierney (2010) and Sedlacek et al. (2014). All data are adjusted to NIST SRM 987 = 0.710248 (McArthur et al. 2001). All data are recalculated to the Geologic Time Scale 2012 (Gradstein et al. 2012). Black curve with a grey 95% confidence envelope: Sr look-up table Version 5 (McArthur et al. 2001, 2012); green curve with a light green 95% confidence envelope: Running average of biostratigraphically well-defined (conodont biozonation) and well-preserved (diagenetically screened) brachiopod data from Korte et al. (2006) with 2 myr steps and a 5 myr window. Carbon., Carboniferous; Pennsylv, Pennsylvanian; Ch., Changhsingian; Ind., Induan; Olen., Olenekian.

The Early–Middle Permian downwards trend of the marine $^{87}Sr/^{86}Sr$ curve has been used to improve age constraints in multiple localities: for example, Japan (Miura et al. 2004), Russia (Nurgalieva et al. 2007), Spitsbergen (Ehrenberg

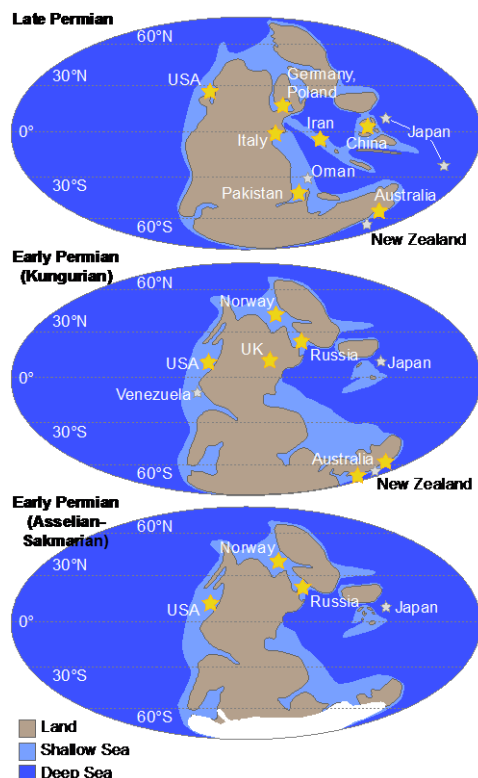et al. 2010), Oman (Stephenson et al. 2012) and Venezuela (Laya et al. 2013)

Fig. 3. Palaeogeographical maps with sample localities for the Asselian–Sakmarian (c. 299–290 Ma), Kungurian (c. 284–272 Ma) and Wuchiapingian–Changhsingian (c. 260–252 Ma) interval. Maps modified from Metcalfe (2011). Yellow stars depict regions studied to constrain the marine ^{87}Sr/^{86}Sr curve for the respective intervals. Grey stars denote studied regions for which ^{87}Sr/^{86}Sr analyses were used to either estimate depositional ages or where age constraints are too weak to precisely define sample age.

The Capitanian ^{87}Sr/^{86}Sr minimum

The Pennsylvanian–Guadalupian (c. 313–262 Ma: McArthur et al. 2012) (Fig. 2) trend of decreasing ^{87}Sr/^{86}Sr stops in the Capitanian (late Guadalupian) at ratios of approximately 0.7068–0.7069 (Burke et al. 1982; Denison et al. 1994; Morante 1996; Korte et al. 2006; Kani et al. 2008, 2013; Wignall et al. 2009; Shen et al. 2010; Tierney 2010; Liu et al. 2013). These low values are the lowest recorded for the entire Palaeozoic and very close to the Phanerozoic minimum at the Middle–Late Jurassic transition (Jones et al. 1994; McArthur et al. 2012), and therefore an important chemostratigraphic marker. The Capitanian minimum has consequently been used as a stratigraphic marker: for example, in carbonate successions now exposed in China (Huang et al. 2008) and Japan (Kani et al. 2008, 2013).

The Wuchiapingian–Changhsingian increasing ^{87}Sr/^{86}Sr trend

The ^{87}Sr/^{86}Sr ratios for the Late Permian and the P–Tr boundary were obtained from different archives: magnesites of the Eastern Alps (Frimmel & Niedermayr 1991); evaporites (Kampschulte et al. 1998; Denison & Peryt 2009) for the Zechstein of the Germanic Basin; gypsum and anhydrite for several North Alpine localities (Spötl & Pak 1996), and bulk carbonate for the Gartnerkofel core (Austria) (Kralik 1991); and at the GSSP site at Meishan in China (Kaiho et al. 2001; Cao et al. 2009). Records of ^{87}Sr/^{86}Sr across the P–Tr boundary, obtained solely from conodonts, were published for different sections of the Salt Range (Pakistan) (Martin&Macdougall 1995), for Abadeh (Iran) and Sosio (Italy) (Korte et al. 2003, 2004), and for Meishan (Twitchett 2007). Late Permian ^{87}Sr/^{86}Sr ratios of well-preserved brachiopods have been reported by Gruszczynski et al. (1992) and Stemmerik et al. (2001) for high-latitude localities from Greenland and Spitsbergen, and by Korte et al. (2006) for the low-latitude successions (Meishan and other Chinese localities, and Jolfa, Iran). Throughout the Wuchiapingian and Changhsingian (Lopingian = Late Permian), ^{87}Sr/^{86}Sr ratios show a moderate increase that steepens in the latest Permian to its Phanerozoic maximum rate of increase around the P–Tr boundary (Fig. 2) (e.g. Martin & Macdougall 1995; Korte et al. 2003, 2004; McArthur et al. 2012). At the P–Tr boundary, the marine ^{87}Sr/^{86}Sr curve reaches a value of approximately 0.7071–0.7072 (e.g. Korte et al. 2003, 2004, 2006; Sedlacek et al. 2014).

In conodont records, the Late Permian–Early Triassic increasing trend has been observed to be interrupted by a phase of relatively little change in seawater ^{87}Sr/^{86}Sr across the P–Tr boundary (Twitchett 2007; Korte et al. 2010) (Fig. 4). This interruption of the long-term trend has been suggested to last from the early Dorashamian (Changhsingian) up to the higher Induan I. isarcica Zone (Fig. 4). In bulk carbonate records from Meishan, however, a general positive ^{87}Sr/^{86}Sr trend is visible in the same interval (Kaiho et al. 2001), but not in acetic acid leachates from carbonates of the same area (Cao et al. 2009). Dubious data related to diagenesis are evident in whole-rock datasets: for example, contradictory values just below the event horizon (Meishan bed 21: c. 0.708 (Kaiho et al. 2001) v. c. 0.7072 (Cao et al. 2009)). The samples of Cao et al. (2009) originate from a core rather than from the deeply weathered outcrops at Meishan. The core-derived ^{87}Sr/^{86}Sr values are similar to those of the conodonts from Iran (Korte et al. 2004) and may therefore represent

the primary past seawater signal more closely. A transient ^{87}Sr/^{86}Sr positive bulge of approximately 0.0008 in the Meishan-1 core throughout the lower half of the Griesbachian (early Induan stage), however, also indicates some preservation issues within this record.

Up to the early Middle Triassic, ^{87}Sr/^{86}Sr values continue to rise (Martin & Macdougall 1995; Korte et al. 2003; McArthur et al. 2012), reaching a maximum value of approximately 0.7080 – similar to the value at the Carboniferous–Permian boundary.

Age resolution of the Permian ^{87}Sr/^{86}Sr curve

The marine ^{87}Sr/^{86}Sr curve as, for example, approximated by Howarth & McArthur (1997) and McArthur et al. (2001, 2012) permits the assignment of numerical ages to samples that cannot otherwise be constrained precisely in time owing to a lack of suitable alternative methods. The main factors affecting this potential for deriving stratigraphic information are: (I) the accuracy of the curve; (II) the precision of the curve; (III) its rate of change; (IV) the precision of laboratory analyses; and (V) the fidelity of the ^{87}Sr/^{86}Sr data derived from the materials, the age of which is to be evaluated.

(I) & (II) Biases in the marine ^{87}Sr/^{86}Sr curve of some magnitude have been present and will persist unless the evolution of seawater can be constrained more tightly through a renewed effort in covering the entire Phanerozoic with multiple high-quality, high-resolution ^{87}Sr/^{86}Sr datasets. For the Permian period, the Artinskian–Wordian interval is currently especially underconstrained and has yielded conflicting proxy data (Fig. 2). The precision of the often-employed strontium look-up table (Howarth & McArthur 1997; McArthur et al. 2001) is only given by the uncertainty of the LOWESS fit to the data that were chosen for its construction. This precision should therefore not be taken as meaningful for either confidence in the curve or for results obtained from measuring ^{87}Sr/^{86}Sr ratios of unknown materials (see also McArthur et al. 2001, 2012).

(III) & (IV) The faster the seawater ^{87}Sr/^{86}Sr ratio changed through time, the higher the theoretical resolution that can be expected, as long as this change is unidirectional, as seen, for example, since the late Eocene (see also McArthur et al. 2012 for an overview). Ignoring artefacts of diagenesis and biases in the ^{87}Sr/^{86}Sr curve, the age resolution of a datum is given as the ratio of analytical uncertainty with the rate of change of the marine ^{87}Sr/^{86}Sr curve (0.000035 per myr on average in the Permian). Except for the steepening Changhsingian ^{87}Sr/^{86}Sr increase leading up to the fastest observed rate of change

in the Phanerozoic in the Early Triassic, the marine ^{87}Sr/^{86}Sr ratio appears to have changed throughout the Permian at a rate that is quite typical for the Phanerozoic (McArthur et al. 2012). From this rate of change, an average age resolution of 0.6 myr for a typical uncertainty value of 0.000020 can be expected for the whole period (Table 1). The Artinskian fares worst, with a rate of change of approximately 0.000011 per myr, whereas the Changhsingian is characterized by a very rapid rate of change of approximately 0.00011 per myr, leading to the best nominal resolution.

(V) The above calculations yield encouragingly high nominal temporal precision – especially when new, high-precision laboratory protocols are implemented. Such numbers, however, are unrealistic: besides the high likelihood that the best estimate of the marine ^{87}Sr/^{86}Sr curve is wrong in places (the curve can only be as good as the data taken to constrain it), the uncertainty of fossil ^{87}Sr/^{86}Sr ratios is never defined by analytical precision alone. A crude test for this effect is illustrated in Table 1. Here the median deviation of a datum from the ^{87}Sr/^{86}Sr reference curve (Sr look-up table Version 5: McArthur et al. 2001, 2012) for brachiopod samples that have passed screening for diagenesis is given for each Permian stage and the whole period.
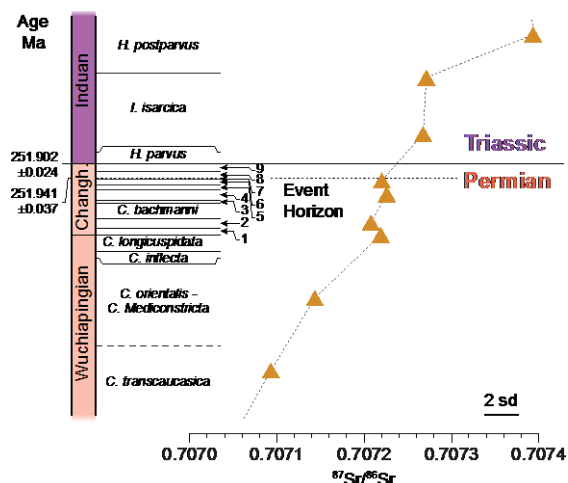

Fig. 4. Wuchiapingian–Induan ^{87}Sr/^{86}Sr record from conodonts at Abadeh, Iran (modified from Korte et al. 2010). 1, C. hambastensis Zone; 2, C. subcarinata Zone; 3, C. nodosa Zone; 4, C. changxingensis–C. deflecta Zone; 5, C. zhangi Zone; 6, C. iranica Zone; 7, C. hauschkei Zone; 8, C. meishanensis–H. praeparvus Zone; 9, M. ultima–S. ?mostleri Zone; Changh., Changhsingian; EH, event horizon. Ages are from Burgess et al. (2014).

The resulting deviations are only comparable to the nominal age resolution of the reference curve where it has been constructed from the same samples used here to test its resolution.

7

Otherwise, median age disagreements up to 8 times as large (almost 9 myr for the Kungurian) and 2.3 myr (4 times worse than nominal resolution) for the whole Permian are observed. To counteract this inherent noise in the fossil data, it is therefore not enough to measure single $^{87}Sr/^{86}Sr$ data for age determination. Instead, multiple analyses and site-specific studies of magnitude and direction of isotopic change through post-depositional processes are paramount for robust age estimates.

Geological interpretation of the Permian $^{87}Sr/^{86}Sr$ curve

Contrasting conclusions have been drawn about the $^{87}Sr/^{86}Sr$ evolution of the Permian due to the use of different carbonate archives. Bulk carbonate samples are readily available, for example, from the best-studied P–Tr boundary sequences, and allow determination of the $^{87}Sr/^{86}Sr$ ratio at superior stratigraphic resolution. Their susceptibility for diagenetic alteration, however, often makes it hard to assess data quality objectively. Confidence in $^{87}Sr/^{86}Sr$ ratios of fossil materials can be bolstered by testing preservation through various geochemical and optical techniques. Phosphatic conodonts and low-Mg calcitic brachiopods have therefore played a major role in constraining the Permian $^{87}Sr/^{86}Sr$ curve. Their occurrence, however, is bound to certain depositional environments and, especially during biotic crises, the quality and abundance of fossils deteriorates dramatically. For example, brachiopods can only found on very rare occasions in earliest Triassic strata. Erroneous inferences about past seawater $^{87}Sr/^{86}Sr$ can therefore primarily arise from unconstrained amounts of alteration in bulk rock records, and from data sparsity and minor diagenetic effects in macrofossil records.

The geological interpretation of the marine $^{87}Sr/^{86}Sr$ curve faces the additional problem of an underconstrained system, where flux magnitudes and isotopic ratios of strontium sources to the ocean and the net effect of geological processes on these parameters are not well known. It is, furthermore, doubtful that the marine $^{87}Sr/^{86}Sr$ ratios have ever reached a dynamic equilibrium – a prerequisite for interpreting absolute changes in the $^{87}Sr/^{86}Sr$ curve. Evaluation of the modern situation rather suggests that the Sr cycle is out of equilibrium (e.g. Pearce et al. 2015) and it may be instructive to also evaluate relevant forcings leading to changes in the slope of the $^{87}Sr/^{86}Sr$ curve. Explaining the marine $^{87}Sr/^{86}Sr$ in a tectonic or palaeoenvironmental framework therefore most often remains conjecture, but can constitute one of multiple lines of evidence for reconstructing models of past Earth systems.

The Early–Middle Permian trend

Few studies have addressed the geological significance of the Early–Middle Permian decrease in seawater $^{87}Sr/^{86}Sr$. Initially, this decrease was related to enhanced igneous activity (Denison et al. 1994). A later interpretation put forward a combination of the Permian–Carboniferous glaciation, Early–Middle Permian aridity and enhanced seafloor spreading related to the opening of the Neotethys (Korte et al. 2006). In particular, the change from 'worldwide' generally more humid conditions in the Asselian and early Sakmarian – suggested by widespread coal seams in Gondwana and the wet climate in the Euramerian province – to progressively more arid conditions (e.g. 'White Band' of South Africa: Kozur 1984) predominantly during the Artinskian and Kungurian have been pointed out (Korte et al. 2006). The associated decrease in chemical weathering and probable reduction in radiogenic riverine Sr fluxes can explain well the evolution of the strontium isotope curve.

Table 1. Theoretical and practical age resolution of the Permian $^{87}Sr/^{86}Sr$ curve

Stage	avg. rate of change per Ma	nominal time resolution Ma
Changhsingian	0.000109	0.2
Wuchiapingian	0.000029	0.7
Capitanian	0.000032	0.6
Wordian	0.000063	0.3
Roadian	0.000025	0.8
Kungurian	0.000019	1.1
Artinskian	0.000011	1.9
Sakmarian	0.000056	0.4
Asselian	0.000063	0.3
Permian	0.000035	0.6

The nominal age resolution is computed assuming an analytical uncertainty of +0.00002. Median deviations of published data and number of published data are from screened brachiopods.

The Capitanian $^{87}Sr/^{86}Sr$ minimum

The $^{87}Sr/^{86}Sr$ minimum of the Capitanian has received ample attention in the literature (e.g. Huang et al. 2008; Kani et al. 2008, 2013; Isozaki 2009; Wignall et al. 2009). The Capitanian turning point has been related to the initiation of the Pangaea break-up (Kani et al. 2008), a mantle plume (Isozaki 2009), cessation of basaltic volcanism, the humidification of Pangaea (Korte et al. 2006; Wignall et al. 2009), or deglaciation and continental doming (Kani et al. 2013).

Late Permian–Early Triassic trend

The increase of marine $^{87}Sr/^{86}Sr$ ratios commencing in the Capitanian has received attention because it reaches a steepness apparently not matched at any other time in the Phanerozoic (McArthur et al. 2012). It has been pointed out, however, that the exact slope is subject to uncertainties in the absolute interval of time recorded by the Late Permian–Early Triassic strata and might, therefore, be overestimated (Denison&Koepnick 1995;

McArthur et al. 2012; see also Korte et al. 2003). The $^{87}Sr/^{86}Sr$ increase has been explained by changes in the Sr cycle, namely a combination of increasing riverine Sr flux, an increasing riverine $^{87}Sr/^{86}Sr$ ratio and a reduction in hydrothermal Sr flux commencing in the Wordian–Capitanian (Martin & Macdougall 1995; see also Morante 1996). The latest Permian destruction of dense land vegetation and associated enhanced continental erosion that lasted until the Anisian has been put forward as an additional influence (Korte et al. 2003; Huang et al. 2008).

Permian–Triassic boundary

An intermittent retardation of the generally increasing Late Permian–Early Triassic $^{87}Sr/^{86}Sr$ trend at the P–Tr boundary has been suggested on the grounds of Permian brachiopod (Korte et al. 2006) and conodont data (Korte et al. 2010) (Fig. 4). Whilst its presence is still a matter of debate, a relatively short-lived (a few 100 kyrs) modulation of the marine $^{87}Sr/^{86}Sr$ curve would have potentially far-reaching implications for the latest Permian Earth system behaviour. Such retardation requires temporary changes in the balance of Sr fluxes or in the $^{87}Sr/^{86}Sr$ ratio of riverine runoff. This change in balance could be related to either: (1) a relative decrease in the riverine Sr flux, by a reduced weathering and hydrological cycle or increased mid-ocean ridge activity; or (2) a lowering of the $^{87}Sr/^{86}Sr$ ratio of continental runoff.

A reduction in the continental Sr flux could be related to global sea-level change, altering the contribution of Sr from continental weathering. Global sea-level rise, however, starts no earlier than the late Changhsingian C. hauschkei Zone, distinctly later than the anticipated change in slope of the seawater $^{87}Sr/^{86}Sr$ curve. A change in slope of the Sr-isotope curve related to a decrease in the river flux to the oceans is also at odds with sedimentological and geochemical evidence (Twitchett 2007). Geochemical records rather suggest an increase in the river discharge in several regions. The Germanic Basin (Kozur 1998a, b), Russia (Newell et al. 1999), South Africa (Ward et al. 2000) and eastern Australia (Michaelsen 2002) all show this effect, but detailed correlation of facies changes in the latter three with the Germanic Basin is not feasible. Twitchett (2007) therefore suggested instead that a change in river water $^{87}Sr/^{86}Sr$ ratios towards less radiogenic Sr may have been generated by enhanced weathering of carbonates or evaporites due to catchment extension. Also, large amounts of strontium from basaltic rocks of the Siberian Traps would have been supplied to the oceans by rapid weathering (Holser & Magaritz 1987; Grard et al. 2005). In addition,

volcanic aerosols causing acid rain may have accelerated weathering rates (Kozur 1998a, b; Krassilov & Karasev 2009; Korte & Kozur 2010; Korte et al. 2010; see also Visscher et al. 2004; Sephton et al. 2005; Wignall 2007; Kraus et al. 2013; Schobben et al. 2014; Sedlacek et al. 2014).

These processes, forcing the global continental runoff to less radiogenic $^{87}Sr/^{86}Sr$ ratios, may match temporally and might, therefore, be the cause of the interruption in the seawater $^{87}Sr/^{86}Sr$ increase at the P–Tr boundary (Korte et al. 2010). Age data for the Siberian trap volcanism, however, are currently not available at high precision and fidelity (Burgess et al. 2014), and it has been suggested that the hypothetical transient interruption of the seawater $^{87}Sr/^{86}Sr$ increase precedes the onset of volcanism (Korte et al. 2010). A direct connection between volcanic forcing and the $^{87}Sr/^{86}Sr$ response can therefore only be made ambiguously. In addition, ε_{Nd} values in this interval in records for Pakistan and the USA (Martin & Macdougall 1995) indicate an intensified Nd contribution of old continental crust to the local seawater, which predicts an enhanced flux of radiogenic Sr.

Conclusions

The Permian marine $^{87}Sr/^{86}Sr$ curve is trough-shaped, falling from the Moscovian Stage to the Capitanian Stage and subsequently rising to the Middle Triassic Anisian Stage. The falling limb constitutes the strongest sustained decrease in marine $^{87}Sr/^{86}Sr$ ratios of the Phanerozoic and reaches values close the Phanerozoic minimum. The following increase accelerates in the Late Permian, reaching a rate of increase around the P–Tr boundary that is unique in the Phanerozoic.

The $^{87}Sr/^{86}Sr$ ratios of marine fossils are an important chemostratigraphic tool for the correlation of Permian strata, and a precision of approximately ±2 myr can be expected from single analyses for this period.

Geological interpretation of marine $^{87}Sr/^{86}Sr$ ratios through the Permian interval is still problematic owing to partially contradictory published $^{87}Sr/^{86}Sr$ records and the sparsity of available data. Further refinement of the Permian $^{87}Sr/^{86}Sr$ trend is necessary before less ambiguous interpretations of its significance are possible.

References

Blake, R.E., O'Neil, J.R. & Garcia, G. 1997. Oxygen isotope systematics of biologically mediated reactions of phosphate; I, Microbial degradation of organophosphorus compounds. Geochimica et Cosmochimica Acta, 61, 4411–4422.

Brand, U. 1991. Strontium isotope diagenesis of biogenic aragonite and low-Mg calcite. Geochimica et Cosmochimica Acta, 55, 505–513.

Brand, U. & Veizer, J. 1980. Chemical diagenesis of a multicomponent carbonate system2 1: trace elements. Journal of Sedimentary Petrology, 50, 1219–1236.

Brand, U., Logan, A., Hiller, N. & Richardson, J. 2003. Geochemistry of modern brachiopods: applications and implications for oceanography and paleoceanography. Chemical Geology, 198, 305–334.

Brookins, D.G. 1988. Seawater 87Sr/86Sr for the Late Permian Delaware Basin evaporates (New Mexico, U.S.A.). Chemical Geology, 69, 209–214.

Bruckschen, P., Oesmann, S. & Veizer, J. 1999. Isotope stratigraphy of the European Carboniferous: proxy signals for ocean chemistry, climate and tectonics. Chemical Geology, 161, 127–163.

Bryant, J.D., Jones, D.S. & Mueller, P.A. 1995. Influence of freshwater flux on 87Sr/86Sr chronostratigraphy in marginal marine environments and dating of vertebrate and invertebrate faunas. Journal of Paleontology, 69, 1–6.

Burgess, S.D., Bowring, S. & Shen, S.-Z. 2014. Highprecision timeline for Earth's most severe extinction. Proceedings of the National Academy of Sciences of the United States of America, 111, 3316–3321.

Burke, W.H., Denison, R.E., Hetherington, E.A., Koepnick, R.B., Nelson, H.F. & Otto, J.B. 1982. Variation of seawater 87Sr/86Sr throughout Phanerozoic time. Geology, 10, 516–519.

Burla, S., Oberli, F., Heimhofer, U., Wiechert, U. & Weissert, H. 2009. Improved time control on Cretaceous coastal deposits: new results from Sr isotope measurements using laser ablation. Terra Nova, 21, 401–409.

Cao, C.-Q., Love, G.D., Hays, L.E., Wang, W., Shen, S.-Z. & Summons, R.E. 2009. Biogeochemical evidence for euxinic oceans and ecological disturbance presaging the end-Permian mass extinction event. Earth and Planetary Science Letters, 281, 188–201.

Denison, R.E. & Koepnick, R.B. 1995. Variations in 87Sr/86Sr of Permian seawater: an overview. In: Scholle, P.A., Peryt, T.M. & Ulmer-Scholle, D.S. (eds) The Permian of Northern Pangea. Springer, Berlin, 124–132.

Denison, R.E. & Peryt, T.M. 2009. Strontium isotopes in the Zechstein (Upper Permian) anhydrites of Poland: evidence of varied meteoric contributions to marine brines. Geological Quarterly, 53, 159–166.

Denison, R.E., Koepnick, R.B., Burke, W.H., Hetherington, E.A. & Fletcher, A. 1994.Construction of the Mississippian, Pennsylvanian and Permian seawater 87Sr/86Sr curve. Chemical Geology, 112, 146–167.

Denison, R.E., Miller, N.R., Scott, R.W. & Reaser, D.F. 2003. Strontium isotope stratigraphy of the Comanchean Series in north Texas and southern Oklahoma. Geological Society of America Bulletin, 115, 669–682.

DePaolo, D.J. & Ingram, B.L. 1985. High-resolution stratigraphy with strontium isotopes. Science, 227, 938–941.

Diener, A., Ebneth, S., Veizer, J. & Buhl, D. 1996. Strontium isotope stratigraphy of the middle Devonian: brachiopods and conodonts. Geochimica et Cosmochimia Acta, 60, 639–652.

Ebneth, S., Diener, A., Buhl, D. & Veizer, J. 1997. Strontium isotope systematics of conodonts: Middle Devonian, Eifel Mountains, Germany. Palaeogeography, Palaeoclimatology, Palaeoecology, 132, 79–96.

Ehrenberg, S.N., McArthur, J.M. & Thirwall, M.F. 2010. Strontium isotope dating of spiculitic Permian strata from Spitsbergen outcrops and Barents Sea wellcores. Journal of Petroleum Geology, 33, 247–254.

Elderfield, H. 1986. Strontium isotope stratigraphy. Palaeogeography, Palaeoclimatology, Palaeoecology, 57, 71–90.

Fischer, J., Schneider, J.W. et al. 2014. Stable and radiogenic isotope analyses on shark teeth from the Early to the Middle Permian (Sakmarian–Roadian) of the southwestern USA. Historical Biology, 26, 710–727.

Frimmel, H.E.E. & Niedermayr, G. 1991. Strontium isotopes in magnesites from Permian and Triassic strata, Eastern Alps. Applied Geochemistry, 6, 89–96.

Gradstein, F.M., Ogg, G. & Schmitz, M. 2012. The Geologic Time Scale 2012, Volumes 1 and 2. Elsevier, Amsterdam.

Grard, A., Franç‚ois, L.M., Dessert, C., Dupré, B. & Godderis, Y. 2005. Basaltic volcanism and mass extinction at the Permo-Triassic boundary: environmental impact and modelling of the global carbon cycle. Earth and Planetary Science Letters, 234, 207–221.

Gruszczynski, M., Hoffman, A., Małkowski, K. & Veizer, J. 1992. Seawater strontium isotopic perturbations at the Permian-Triassic boundary, West Spitsbergen, and its implications for the interpretation of strontium isotopic data. Geology, 20, 779–782.

Hans, U., Kleine, T. & Bourdon, B. 2013. Rb–Sr chronology of volatile depletion in differentiated protoplanets: BABI, ADOR and ALL revisited. Earth and Planetary Science Letters, 374, 204–214.

Henderson, C.M., Davydov, V.I. & Wardlaw, B.R. 2012. The Permian period. In: Gradstein, F.M., Ogg, G. & Schmitz, M. (eds) The Geologic Time Scale 2012, Volume 2. Elsevier, Amsterdam, 653–679.

Hodell, D.A., Mueller, P.A., McKenzie, J.A. & Mead, G.A. 1989. Strontium isotope stratigraphy and geochemistry of the late Neogene ocean. Earth and Planetary Science Letters, 92, 165–178.

Hodell, D.A., Mueller, P.A. & Garrido, J.R. 1991. Variations in the strontium isotopic composition of seawater during the Neogene. Geology, 19, 24–27.

Holser, W.T. & Magaritz, M. 1987. Events near the Permian–Triassic boundary. Modern Geology, 11, 155–180.

Howarth, R.J. & McArthur, J.M. 1997. Statistics for strontium isotope stratigraphy: a robust LOWESS fit to the marine Sr-isotope curve for 0 to 206 Ma, with look-up table for derivation of numeric age. Journal of Geology, 105, 441–456.

Huang, S.-J., Qing, H.-R., Huang, P.-P., Hu, Z.-W., Wang, Q.-D., Zou, M.-L. & Liu, H.-N. 2008. Evolution of strontium isotopic composition of seawater from Late Permian to Early Triassic based on study of marine carbonates, Zhongliang Mountain, Chongqing, China. Science in China Series D: Earth Sciences, 51, 528–539.

Isozaki, Y. 2009. Illawarra Reversal: the fingerprint of a superplume that triggered Pangean breakup and the end-Guadalupian (Permian) mass exctinction. Gondwana Research, 15, 421–432.

Jenkyns, H.C., Jones, C.E., Gröcke, D.R., Hesselbo, S.P. & Parkinson, D.N. 2002. Chemostratigraphy of the Jurassic System: applications, limitations and implications of palaeoceanography. Journal of the Geological Society, London, 159, 351–378, https:// doi.org/10.1144/0016-764901-130

Jones, C.E., Jenkyns, H.C., Coe, A.L. & Hesselbo, S.P. 1994. Strontium isotopic variations in Jurassic and Cretaceous seawater. Geochimica et Cosmochimia Acta, 58, 3061–3074.

Kaiho, K., Kajiwara, Y. et al. 2001. End-Permian catastrophe by a bolide impact: evidence of a gigantic release of sulfur from the mantle. Geology, 29, 815–818.

Kampschulte, A., Buhl, D. & Strauss, H. 1998. The sulfur and strontium isotopic compositions of Permian evaporates from the Zechstein basin, northern Germany. Geologische Rundschau, 87, 192–199.

Kani, T., Fukui, M., Isozaki, Y. & Nohda, S. 2008. The Paleozoic minimum of $^{87}Sr/^{86}Sr$ ratio in the Capitanian (Permian) mid-oceanic carbonates: a critical turning point in the Late Paleozoic. Journal of Asian Earth Sciences, 32, 22–33.

Kani, T., Hisanabe, C. & Isozaki, Y. 2013. The Capitanian (Permian) minimum of $^{87}Sr/^{86}Sr$ ratio in the mid-Panthalassan paleo-atoll carbonates and its demise by deglatiation and continental doming. Gondwana Research, 24, 212–221.

Korte, C. & Kozur, H.W. 2010. Carbon-isotope stratigraphy across the Permian–Triassic boundary: a review. Journal of Asian Earth Sciences, 39, 215–235.

Korte, C., Kozur, H.W., Bruckschen, P. & Veizer, J. 2003. Strontium isotope evolution of Late Permian and Triassic seawater. Geochimica et Cosmochimica Acta, 67, 47–62.

Korte, C., Kozur, H.W., Joachimski, M.M., Strauss, H., Veizer, J. & Schark, L. 2004. Carbon, sulfur, oxygen and strontium isotope records, organic geochemistry and biostratigraphy across the Permian/Triassic boundary in Abadeh, Iran. International Journal of Earth Sciences, 93, 565–581.

Korte, C., Jasper, T., Kozur, H.W. & Veizer, J. 2006. $^{87}Sr/^{86}Sr$ record of Permian seawater. Palaeogeography, Palaeoclimatology, Palaeoecology, 240, 89–107.

Korte, C., Pande, P., Kalia, P., Kozur, H.W., Joachimski, M.M. & Oberhänsli, H. 2010. Massive volcanism at the Permian-Triassic boundary and its impact on the isotopic composition of the ocean and atmosphere. Journal of Asian Earth Sciences, 37, 293–311.

Kozur, H. 1984. Perm. In: Tröger, K.-A. (ed.) Abriß der Historischen Geologie. Akademie, Berlin, 270–307.

Kozur, H.W. 1998a. Some aspects of the Permian– Triassic boundary (PTB) and of the possible causes for the biotic crisis around this boundary. Palaeogeography, Palaeoclimatology, Palaeoecology, 143, 227–272.

Kozur, H.W. 1998b. Problems for evaluations of the scenario of the Permian–Triassic boundary biotic crisis and of its causes. Geologia Croatica, 51, 135–162.

Kralik, M. 1991. The Permian–Triassic of the Gartnerkofel-1 core (Carnic Alps, Austria): strontium isotopes and carbonate chemistry. Abhandlungen der Geologischen Bundesanstalt in Wien, 45, 169–174.

Kramm, U. & Wedepohl, K.H. 1991. The isotopic composition of strontium and sulfur in seawater of Late Permian (Zechstein) age. Chemical Geology, 90, 253–262.

Krassilov, V. & Karasev, E. 2009. Paleofloristic evidence of climate change near and beyond the Permian-Triassic boundary. Palaeogeography, Palaeoclimatology, Palaeoecology, 284, 326–336.

Kraus, S.H., Brandner, R., Heubeck, C., Kozur, H.W., Struck, U. & Korte, C. 2013. Carbon isotope signatures of latest Permian marine successions of the Southern Alps suggest a continental runoff pulse enriched in land plant material. Fossil Record, 16, 97–109.

Laya, J.C., Tucker, M.E., Gröcke, D.R. & Perez-Huerta, A. 2013. Carbon, oxygen and strontium isotopic composition of low-latitude Permian carbonates (Venezuelan Andes): climate proxies of tropical Pangea. In: Gasiewicz, A. & Słowakiewicz, M. (eds) Palaeozoic Climate Cycles: Their Evolutionary and Sedimentological Impact. Geological Society, London, Special Publications, 376, 367–385, https://doi.org/10.1144/SP376.10

Li, Y.-H. 1982. A brief discussion on the mean oceanic residence time of elements. Geochimica et Cosmochimica Acta, 46, 2671–2675.

Liu, X.-c., Wang, W. et al. 2013. Late Guadalupian to Lopingian (Permian) carbon and strontium isotopic chemostratigraphy in the Abadeh section, central Iran. Gondwana Research, 24, 222–232.

Martin, E.E. & Macdougall, J.D. 1995. Sr and Nd isotopes at the Permian/Triassic boundary: a record of climate change. Chemical Geology, 125, 73–99.

McArthur, J.M. 1994. Recent trends in strontium isotope stratigraphy. Terra Nova, 6, 331–358.

McArthur, J.M., Howarth, R.J. & Bailey, T.R. 2001. Strontium isotope stratigraphy: LOWESS version 3: best fit to the marine Sr-isotope curve for 0–509 Ma and accompanying look-up table for deriving numerical age. Journal of Geology, 109, 155–170.

McArthur, J.M., Howarth, R.J. & Shields, G.A. 2012. Strontium isotope stratigraphy. In: Gradstein, F.M., Ogg, J.G., Schmitz, M. & Ogg, G. (eds) The Geologic Time Scale, Volume 1. Elsevier, Amsterdam, 127–144.

Metcalfe, I. 2011. Tectonic framework and Phanerozoic evolution of Sundaland. Gondwana Research, 19, 3–21.

Michaelsen, P. 2002. Mass extinction of peat-formation plants and the effect on fluvial styles across the Permian–Triassic boundary, northern Bowen Basin, Australia. Palaeogeography, Palaeoclimatology, Palaeoecology, 179, 173–188.

Miura, N., Asahara, Y. & Kawabe, I. 2004. Rare earth element and Sr isotopic study of the Middle Permian limestone–dolostone sequence in Kuzuu area, central Japan: seawater tetrad effect and Sr isotopic signatures of seamount-type carbonate rocks. Journal of Earth and Planetary Sciences, Nagoya University, 51, 11–35.

Morante, R. 1996. Permian and Early Triassic isotopic records of carbon and strontium in Australia and a scenario of events about the Permian-Triassic boundary. Historical Biology, 11, 289–310.

Newell, A.J., Tverdokhlebov, V.P. & Benton, M.J. 1999. Interplay of tectonics and climate on a transverse fluvial system, Upper Permian, Southern Uralian Foreland Basin, Russia. Sedimentary Geology, 127, 11–29.

Neymark, L.A., Premo, W.R., Mel'nikov, N.N. & Emsbo, P. 2014. Precise determination of $d_{88}Sr$ in rocks, minerals, and waters by double-spike TIMS: a powerful tool in the study of geological, hydrological and biological processes. Journal of Analytical Atomic Spectrometry, 29, 65–75.

Nier, A.O. 1938. The isotopic constitution of strontium, barium, bismuth, thallium and mercury. Physical Review, 54, 275–278.

Nishioka, S., Arakawa, Y. & Kobayashi, Y. 1991. Strontium isotope profile of Carboniferous–Permian Akiyoshi Limestone in southwest Japan. Geochemical Journal, 25, 137–146.

Nurgalieva, N.G., Ponomarchuk, V.A. & Nurgaliev, D.K. 2007. Strontium isotope stratigraphy: possible applications for age estimation and global correlation of Late Permian carbonates of the Pechishchi type section, Volga River. Russian Journal of Earth Sciences, 9, ES1002.

Palmer, M.R. & Edmond, J.M. 1989. The strontium isotopic budget of the modern ocean. Earth and Planetary Science Letters, 92, 11–26.

Palmer, M.R. & Elderfield, H. 1985. Sr isotope composition of sea water over the past 75 Myr. Nature, 314, 526–528.

Pearce, C.R., Parkinson, I.J., Gaillardet, J., Charlier, B.L.A., Mokadem, F. & Burton, K.W. 2015. Reassessing the stable ($\delta^{88/86}Sr$) and radiogenic ($^{87}Sr/^{86}Sr$) strontium isotopic composition of marine inputs. Geochimica et Cosmochimica Acta, 157, 125–146.

Peterman, Z.E., Hedge, C.E. & Tourtelot, H.A. 1970. Isotopic composition of strontium in sea water throughout Phanerozoic time. Geochimica et Cosmochimica Acta, 34, 105–120.

Popp, B.N., Anderson, T.F. & Sandberg, P.A. 1986. Brachiopods as indicators of original isotopic compositions in some Paleozoic limestones. Geological Society of America Bulletin, 97, 1262–1269.

Rasmussen, C.M.Ø., Ullmann, C.V. et al. 2016. Onset of main Phanerozoic marine radiation sparked by emerging Mid Ordovician icehouse. Scientific Reports, 6, 18884.

Schobben, M., Joachimski, M.M., Korn, D., Leda, L. & Korte, C. 2014. Palaeotethys seawater temperature rise and an intensified hydrological cycle following the end-Permian mass extinction. Gondwana Research, 26, 675–683.

Sedlacek, A.R.C., Saltzman, M.R., Algeo, T.J., Horacek, M., Brandner, R., Foland, K. & Denniston, R.F. 2014. $^{87}Sr/^{86}Sr$

stratigraphy from the Early Triassic of Zal, Iran: linking temperature to weathering rates and the tempo of ecosystem recovery. Geology, 42, 779–782.

Sephton, M.A., Looy, C.V., Brinkhuis, H., Wignall, P.B., de Leeuw, J.W. & Visscher, H. 2005. Catastrophic soil erosion during the end-Permian biotic crisis. Geology, 33, 941–944.

Sharma, M., Balakrishna, K., Hofmann, A.W. & Shankar, R. 2007. The transport of Osmium and Strontium isotopes through a tropical estuary. Geochimica et Cosmochimica Acta, 71, 4856–4867.

Shen, Shu-zhong, Henderson, C.M. et al. 2010. Highresolution Lopingian (Late Permian) timescale of South China. Geological Journal, 45, 122–134.

Shields, G.A., Carden, G.A.F., Veizer, J., Meidla, T., Rong, J.-Y. & Li, R.-Y. 2003. Sr, C, and O isotope geochemistry of Ordovician brachiopods: a major isotopic event around the Middle-Late Ordovician transition. Geochimica et Cosmochimica Acta, 67, 2005–2025.

Spötl, C. & Pak, E. 1996. A strontium and sulfur isotopic study of Permo-Triassic evaporites in the Northern Calcareous Alps, Austria. Chemical Geology, 131, 219–234.

Steiger, R.H. & Jäger, E. 1977. Subcommission on geochronology: convention on the use of decay constants in geo- and cosmochronology. Earth and Planetary Science Letters, 36, 359–362.

Stemmerik, L., Bendix-Almgreen, S.E. & Piasecki, S. 2001. The Permian-Triassic boundary in central East Greenland: past and present views. Bulletin of the Geological Society of Denmark, 48, 159–167.

Stephenson, M.H., Angiolini, L., Leng, M.J. & Darbyshire, F. 2012. Geochemistry, and carbon, oxygen and strontium isotope composition of brachiopods from the Khuff Formation of Oman and Saudi Arabia. GeoArabia, 17, 61–76.

Steuber, T. 2001. Strontium isotope stratigraphy of Turonian–Campanian Gosau-type rudist formations in the Northern Calcareous and Central Alps (Austria and Germany). Cretaceous Research, 22, 429–441.

Steuber, T. 2003. Strontium isotope stratigraphy of Cretaceous hippuritid rudist bivalves: rates of morphological change and heterochronic evolution. Palaeogeography, Palaeoclimatology, Palaeoecology, 200, 221–243.

Steuber, T. & Schlüüter, M. 2012. Strontium-isotope stratigraphy of Upper Cretaceous rudist bivalves: Biozones, evolutionary patterns and sea-level change calibrated to numerical ages. Earth-Science Reviews, 114, 42–60.

Taylor, A.S. & Lasaga, A.C. 1999. The role of basalt weathering in the Sr isotope budget of the oceans. Chemical Geology, 161, 199–214.

Tierney, K.E. 2010. Carbon and strontium isotope stratigraphy of the Permian from Nevada and China: Implications from an icehouse to greenhouse transition. PhD thesis, Ohio State University.

Twitchett, R.J. 2007. Climate change across the Permian/Triassic boundary. In: Williams, M., Haywood, A.M., Gregory, F.J. & Schmidt, D.N. (eds) Deep- Time Perspective on Climate Change: Marrying the Signal from Computer Models and Biological Proxies. The Micropalaeontological Society, Special Publications. Geological Society, London, 191–200.

Ullmann, C.V. & Korte, C. 2015. Diagenetic alteration in low-Mg calcite from macrofossils: a review. Geological Quarterly, 59, 3–20.

Ullmann, C.V., Campbell, H.J., Frei, R., Hesselbo, S.P., Pogge von Strandmann, P.A.E. & Korte, C. 2013. Partial diagenetic overprint of Late Jurassic belemnites from New Zealand: implications for the preservation potential of δ^7Li values in calcite fossils. Geochimica et Cosmochimica Acta, 120, 80–96.

Ullmann, C.V., Campbell, H.J., Frei, R. & Korte, C. 2014. Geochemical signatures in Late Triassic brachiopods from New Caledonia. New Zealand Journal of Geology and Geophysics, 57, 420–431.

Ullmann, C.V., Frei, R., Korte, C. & Hesselbo, S.P. 2015. Chemical and isotopic architecture of the belemnite rostrum. Geochimica et Cosmochimia Acta, 159, 231–243.

Veizer, J. 1989. Strontium isotopes in seawater through time. Annual Reviews in Earth and Planetary Sciences, 17, 141–167.

Veizer, J. & Compston, W. 1974. 87Sr/86Sr composition of seawater during the Phanerozoic. Geochimica et Cosmochimica Acta, 38, 1461–1484.

Veizer, J., Buhl, D. et al. 1997. Strontium isotope stratigraphy: potential resolution and event correlation. Palaeogeography, Palaeoclimatology, Palaeoecology, 132, 65–77.

Veizer, J., Ala, D. et al. 1999. ^{87}Sr/^{86}Sr, δ^{13}C and δ^{18}O evolution of Phanerozoic seawater. Chemical Geology, 161, 59–88.

Visscher, H., Looy, C.V., Collinson, M.J., Brinkhuis, H., Konijnenburg-van Cittert, J.H.A., Kürschner, W.M. & Sephton, M.A. 2004. Environmental mutagenesis during the end-Permian ecological crisis. Proceedings of the National Academy of Sciences of the United States of America, 101, 12952–12956.

Ward, P.D., Montgomery, D.R. & Smith, R. 2000. Altered river morphology in South Africa related to the Permian–Triassic Extinction. Science, 289, 1740–1743.

Wefer, G. & Berger, W.H. 1991. Isotope paleontology: growth and composition of extant calcareous species. Marine Geology, 100, 207–248.

Wierzbowski, H., Anczkiewicz, R., Bazarnik, J. & Pawlak, J. 2012. Strontium isotope variations in Middle Jurassic (Late Bajocian–Callovian) seawater: implications for Earth's tectonic activity and marine environments. Chemical Geology, 334, 171–181.

Wignall, P.B. 2007. The end-Permian mass extinction – how bad did it get? Geobiology, 5, 303–309.

Wignall, P.B., Védrine, S., Bond, D.P.G., Wang, W., Lai, X.-L., Ali, J.R. & Jiang, H.-S. 2009. Facies analysis and sea-level change at the Guadalupian–Lopingian Global Stratotype (Laibin, South China), and its bearing on the end-Guadalupian mass extinction. Journal of the Geological Society, London, 166, 655–666, https://doi.org/10.1144/0016-76492008-118

Young, E.D. & Galy, A. 2004. The isotope geochemistry and cosmochemistry of magnesium. Reviews in Mineralogy and Geochemistry, 55, 197–230.

Zazzo, A., Lécuyer, C. & Mariotti, A. 2004. Experimentally-controlled carbon and oxygen isotope exchange between bioapatites and water under inorganic and microbially mediated conditions. Geochimica et Cosmochimica Acta, 68, 1–12.